Third International Symposium on the Effects of Surface Geology on Seismic Motion
Grenoble, France, 30 August - 1 September 2006
Paper Number: 064

ACCELEROGRAPH STATIONS SITE CHARACTERIZATION USING AMBIENT NOISE: SELECTED STATIONS IN GREECE

Alexandros SAVVAIDIS[1], Heloise CADET[2], Philippe GUEGUEN[2], Areti PANOU[1], Clotaire MICHEL[2], Nikos THEODULIDIS[1] and Ioannis KALOGERAS[3].
[1] *Institute of Engineering Seismology and Earthquake Engineering, G.Scholis 46, 55102, Thessaloniki, Greece*
[2] *Laboratory of Geophysics and Tectonophysics, BP53, 38041, Grenoble Cedex 09, France*
[3] *Geodynamic Institute, National Observatory of Athens, 20048, 118 10, Athens, Greece*

ABSTRACT – Recent research efforts showed that ambient noise measurements performed either by a single autonomous station or by an array configuration can be used along with a proper methodology to satisfactorily acquire the shear wave velocity profile at a site. The knowledge of shear wave velocity of the subsurface structure at strong motion stations is indispensable since it can significantly optimize the use of existing and future strong motion recordings obtained, rendering them usable to their full potential. Microtremor array measurements have been acquired in six strong motion sites of the national strong motion network in Greece where shear wave velocity information exist at least up to a depth of about 40 m. In two sites, borehole and cross-hole data show the depth of the seismic bedrock. The array geometry used consists of three co-central circles in each site at different apertures. Data have been processed using both F-K and SPAC methods and an inversion of the resulted dispersion curve and auto-correlation data has been followed, respectively. The resulted models are compared with shear wave velocity models from other geophysical methods and the reliability and accuracy of the array method has been evaluated.

1. Introduction

The quantitative assessment of site effects, that is the ground motion effects associated with the local surface geology (among others Borcherdt, 1970; Campell, 1976), is a major issue in engineering seismology studies. Impact and resonance effects of S-waves within unconsolidated sediments overlaying stiffer formations cause frequency dependent site amplifications. Thus, it is of key interest to determine the shallow shear wave velocity structure (Hartzell et al. 1996, Yamanaka 1998). In recent years, the passive recording of microtremors at single stations (among others Bard, 1998; Ishida et al., 1998; Fäh et al., 2003; Arai and Tokimatsu, 2004) or at small-scale arrays (among others Tokimatsu 1997, Scherbaum et al. 2003) has gained considerable attention for the determination of shallow shear wave velocity profiles. The major advantages of these ambient vibration techniques are the low cost exploration and monitoring capabilities, the possibility to perform non-destructive measurements at every place of a densely populated city, and the relatively large penetration depth.

In the present study we apply the array microtremor method in six strong motion sites that in five of them we have earthquake recordings and in all of them we have additional geophysical information from Cross-Hole (CH) data (Pitilakis, 1996; Athanassopoulos et al., 1999; Anastasiadis et al., 2003; Anastasiadis, 2004; Dimitriou et al., 2004). We try to correlate the shear wave velocity, the depth of the first layer and the bedrock calculated from the array data with these calculated from CH data (D_{CH}). Additionally we compare the depth of the bedrock as this is calculated from the resonance frequency from ambient noise recordings (H/V) $D_{HVnoise}$, earthquake data (H/V) D_{HVeq}, and the array data, D_{array}, in order to check the validity of the microtremor array method.

2. Data Used

Microtremor array data were collected at six strong motion sites of the permanent National Strong Motion Network in Greece. The sites used are presented in Figure 1. Three of them correspond to D soil category based on NHERP 1997 (Lefkas/LEF1, Pirgos/PIR1, Korinthos/KOR1) and three of them correspond to C soil category (Patra/PAT2, Vartholomio/VAR1, Aigion/AIG1).

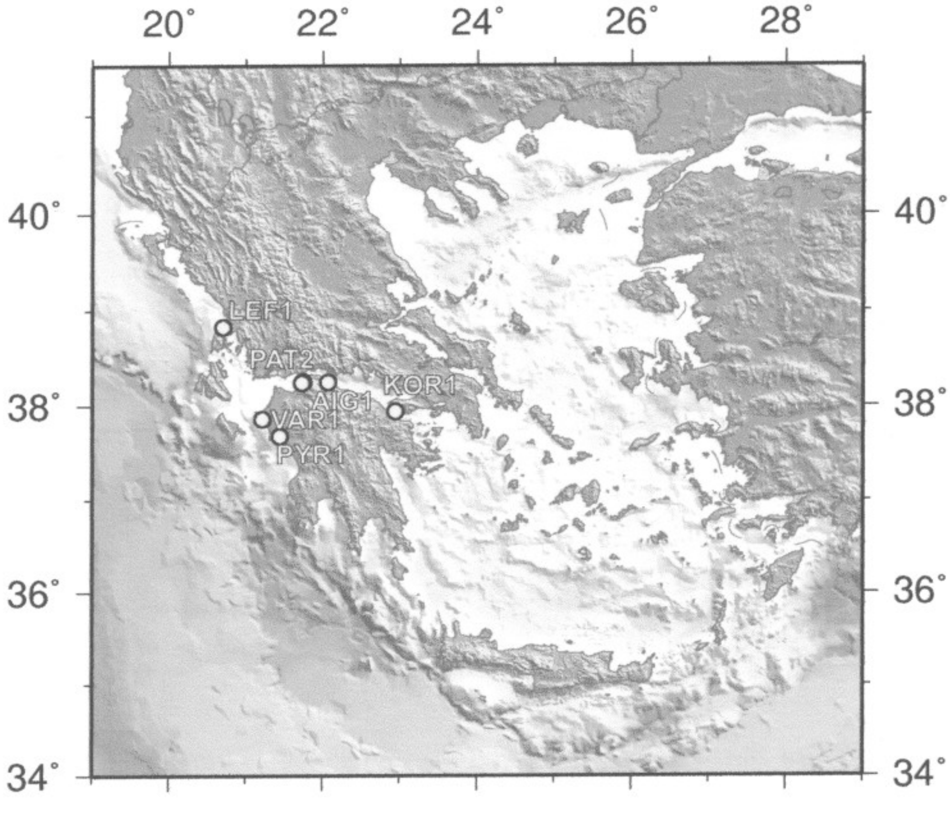

Figure 1. Map of Greece were the sites used during this study are presented.

For the array recordings, Cityshark II, was used with six three-component velocimeters attached (Lennartz 5 sec sensors). Three circles of different apertures were implemented on each site and a recording of 30 minutes to 1 hour was established depending on the aperture of the array. Long recordings were used for larger apertures and short recordings for smaller apertures. One station was located in the center of the site and the other five at approximately 72 degrees angles between them, depending on the building environment and nearby local sources of each site.

The aperture of each circle was selected based on the fundamental frequency at each site, from earthquake or/and individual noise recordings, and known shear wave velocity information up to a depth of at least 40 meters from Cross Hole data. An example of geometry adopted for station KOR1 is presented in Figure 2.

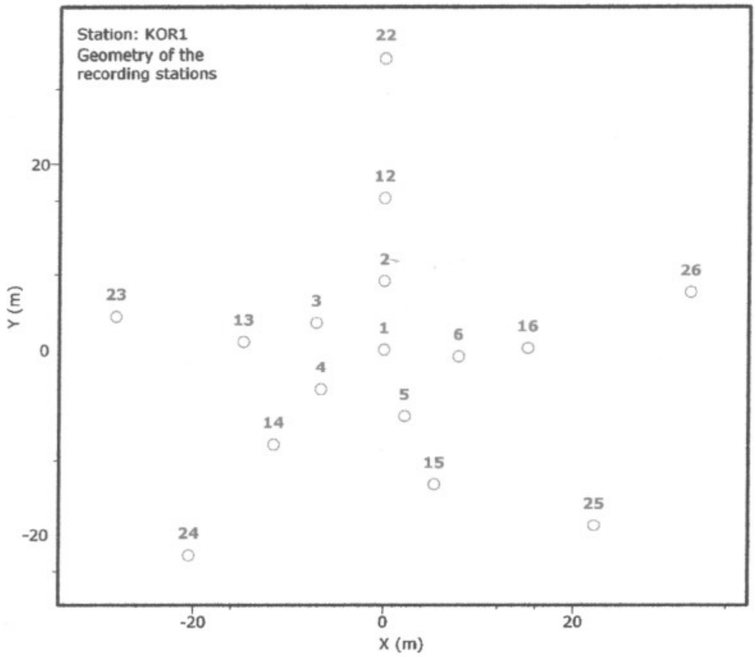

Figure 2. Geometry adopted in the field for microtremor array measurements for the site of KOR1. (1 central station, 2-6 inner circle, 12-16 middle circle, 22-26 outer circle)

3. Processing of Data

To homogeneously process earthquake data and calculate the receiver function (RF), the JSESAME software modules (SESAME European project, 2004a, 2004b) was applied. The entire recording length was taken, ranging from about 10sec to 40sec (Theodulidis et al., 2006).

The following steps were applied to all data used: (a) offset correction, (b) computation of Fourier spectra in all three components (E–W, N–S, UP), (c) application of a cosine taper, (d) smoothing of the Fourier amplitude spectra by a Konno-Ohmachi algorithm (Konno and Ohmachi, 1998). Data analysis was focused in the frequency range between 0.2 and 20 Hz. For each discrete frequency point the horizontal recording spectrum was divided by the vertical one, separately for both horizontal components. Thus, a common procedure was implemented so that any similarities or differences observed could be attributed to factors other than data processing itself.

Fundamental frequency, f_o, of the RF spectral ratio was visually selected. For the examined stations two rough categories of sites with respect to f_o, are observed. One including the stations Korinthos, Lefkas, Patra with f_o equal or higher than 3.0Hz and another the stations Aigio, Vartholomio, Pirgos with f_o lower than 2.0Hz.

Before the processing of the array data, H/V calculations were implemented for all stations of each site as individual recordings in order to estimate a prominent peak corresponding to the fundamental frequency. The same computational parameters were used for H/V calculations for all stations by the SES-ARRAY software (Wathelet et al., 2005). Using an anti-trigger module of the software along the recorded traces, the stable windows of the signal are detected automatically with the following parameters: Window length: 30 seconds, STA : 1.5 second, LTA : 30.0 seconds, Anti-trigger threshold : 0.3 - 2.0. Similar procedure to that used for earthquake data were applied to ambient noise measurement for the calculations of the fundamental frequency.

Data were processed using mostly the Conventional F-K (CVFK) technique and for some sites the Modified SPAC (MSPAC). The CVFK estimates (Kvaerna and Ringdahl, 1986), in sliding time window manner and narrow frequency bands around a center frequency, the parameters of propagation (direction and slowness) of the most coherent plane wave arrival. A grid search over the wavenumber plane is performed for each frequency in order to calculate the dispersion curve. The SPatial AutoCorrelation(SPAC) method is based on the precondition of a stochastic wavefield that is stationary in both time and space (Aki, 1957). Bettig et al. (2003) suggested a modification of Aki's original SPAC formula (MSPAC), which allows applying the spatial autocorrelation method for non-complete circular array configurations. The modification applied concerns the calculation of the averaged spatial autocorrelation coefficients from station pairs taken from rings of finite thickness instead of a fixed radius that is difficult to be implemented in a building environment.

Depending on the geometry of each circle the theoretical response was calculated in order to define the limitations of resolution and aliasing on the dispersion curve (DC) calculation. An example is presented in Figure 3 where the theoretical response of the inner array (radius of 7.5 m) is shown. On the Frequency/Slowness plot the k_{min} and k_{max} limits are calculated in order to approximately define the boundaries of the DC to be used from each array data set. An attempt to calculate the DC down to the f_o resulted from the H/V of individual noise measurements or earthquake data. However, this was not possible in most of the sites since the building environment did not allow having very big apertures. In Figure 4 the DC calculated using the CVFK method for the middle circle for site KOR1, is presented. The theoretical response, corresponding to the middle circle, based on the geometry adopted is also shown.

4. Inversion of Dispersion Curve and Autocorrelation Data

The inversion code implemented from Wathelet et al., (2004) was used, which employs the neighborhood algorithm (Sambridge, 1999a, 1999b), in order to calculate shear wave velocity models from the DC data. Different attempts were evaluated for two, three, and four layers models in order to achieve the lowest misfit. Also, two layer models with the first layer consisting of five sub-layers following a power law were estimated. In Figure 5 the resulted three layer models are shown as calculated from the inversion of the DC data resulted from applying the CVFK method to the microtremor array data of station VAR1.

Direct inversion of autocorrelation curves as resulted from applying MSPAC in the recorded data was employed using the implementation of Wathlet et al., (2005). The results of the inversion for station VAR1 for a three layers model are presented in Figure 6. The autocorrelation curves are presented in the lower part. The grey dots correspond to the results after the processing and the colored curves correspond to the resulted models after the inversion. The resulted models along with the shear wave velocity profile from the CH data are also presented (upper left part). On the upper right hand side the DC's from the resulted models (color lines), the DC from the resulted model of the CH data and the DC from the processing of the data with the CVFK method, are shown.

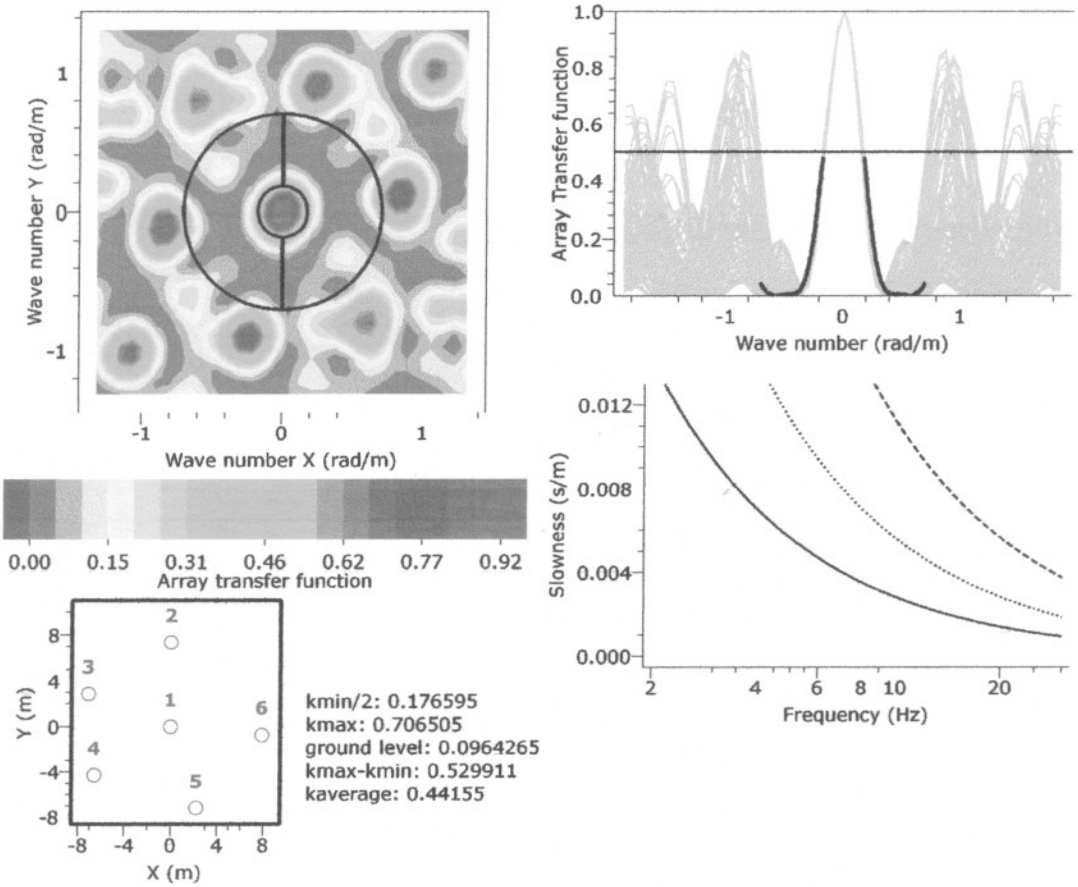

Figure 3. Theoretical Response of the Geometry of the Inner Circle for site KOR1

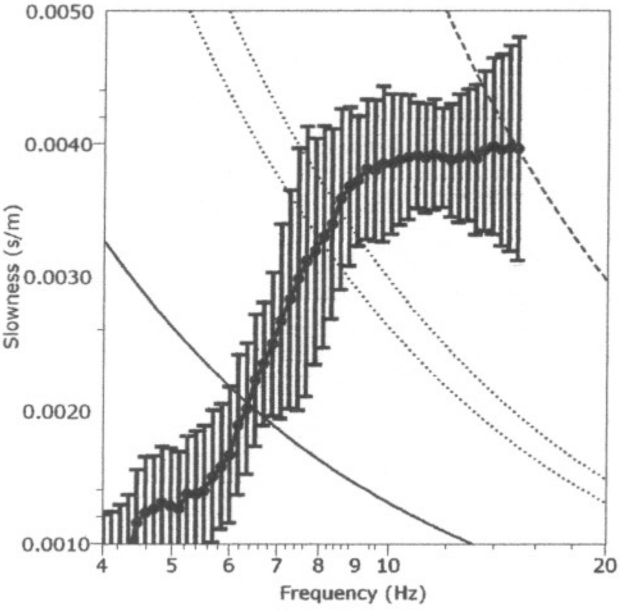

Figure 4. Dispersion curve calculation of the middle circle using CVFK (black dots) with the k_{min} (continuous line) and k_{max} (dashed line) limits plotted from the theoretical response calculation (KOR1).

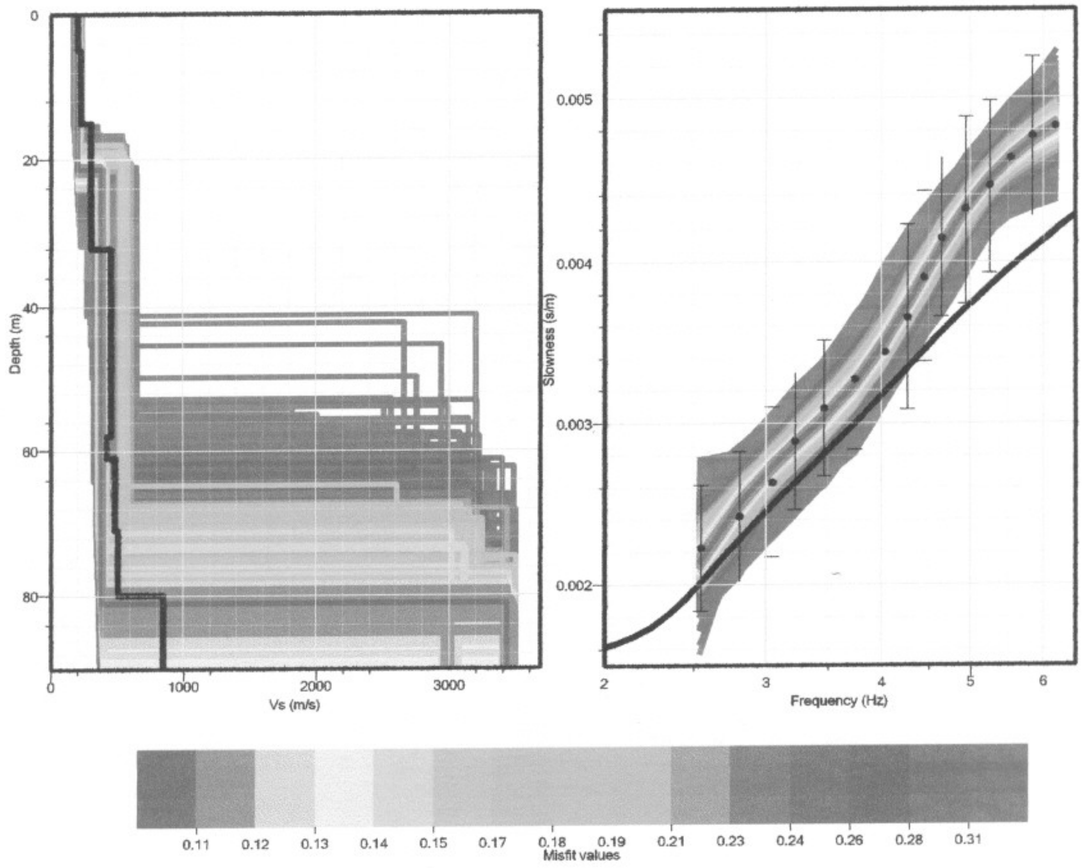

Figure 5. Resulted shear wave velocity model of three layers (left part) resulted from the inversion of the DC (black dots) information (right part). The shear wave velocity model from CH data and its respective DC is also presented with continuous black line (Vartholomio).

5. Discussion

In order to check the subjectivism of calculating shear wave velocity models using the same data set of array data and the same tools, two different teams of people were structured in order to follow a common procedure and check the coherency of their results, presented on Table I. On the first column the name of the site is given, following is the processing method used and the frequency band for which processing was established. On the forth column is the parameter space used for the inversion (2l: two layers model, 2l grad: two layers model with the first layer consisting of five sub-layers that follow a power-law, 3l: three layers model, 3l-2LVL: three layers model with the second one allowing to be a low velocity layer), and following is the shear wave velocity of the first layer (Vs_o) preceded by the values of Vs_o corresponding to resulted models covering -/+ 50% of the standard deviation of the dispersion curve or autocorrelation data. On columns 8-12 different statistical parameters are calculated corresponding to the mean values of Vs_o, $-Vs_o$, $+Vs_o$, and the limit of the shear wave velocity of the first layer in percentage of Vs_o, followed with the spread of data, the depth of the first layer [Ds_o (D_{array})] and the depth to the seismic bedrock [Ds_1(D_{array})]. The above information described is presented for both teams (TEAM A – orange color, TEAM B blue color on Table I). Following, the fundamental frequency ($f(hv)_1$) from H/V of ambient noise data and from earthquake recordings ($f(hv)_2$) are given when this information exists. For each team the

h_{min1} ($D_{HVnoise}$) and h_{min2} (D_{HVeq}) was calculated based on Vs_o and the fundamental frequencies calculated before based on the formula $h_{min}=Vs_o/4f(hv)$. This calculation was implemented for correlating h_{min} with Ds_o or Ds_1 calculated through the inversion. Finally, the coherence between the array results and Cross Hole results for Vs_o and Ds_o or Ds_1 are presented for each team.

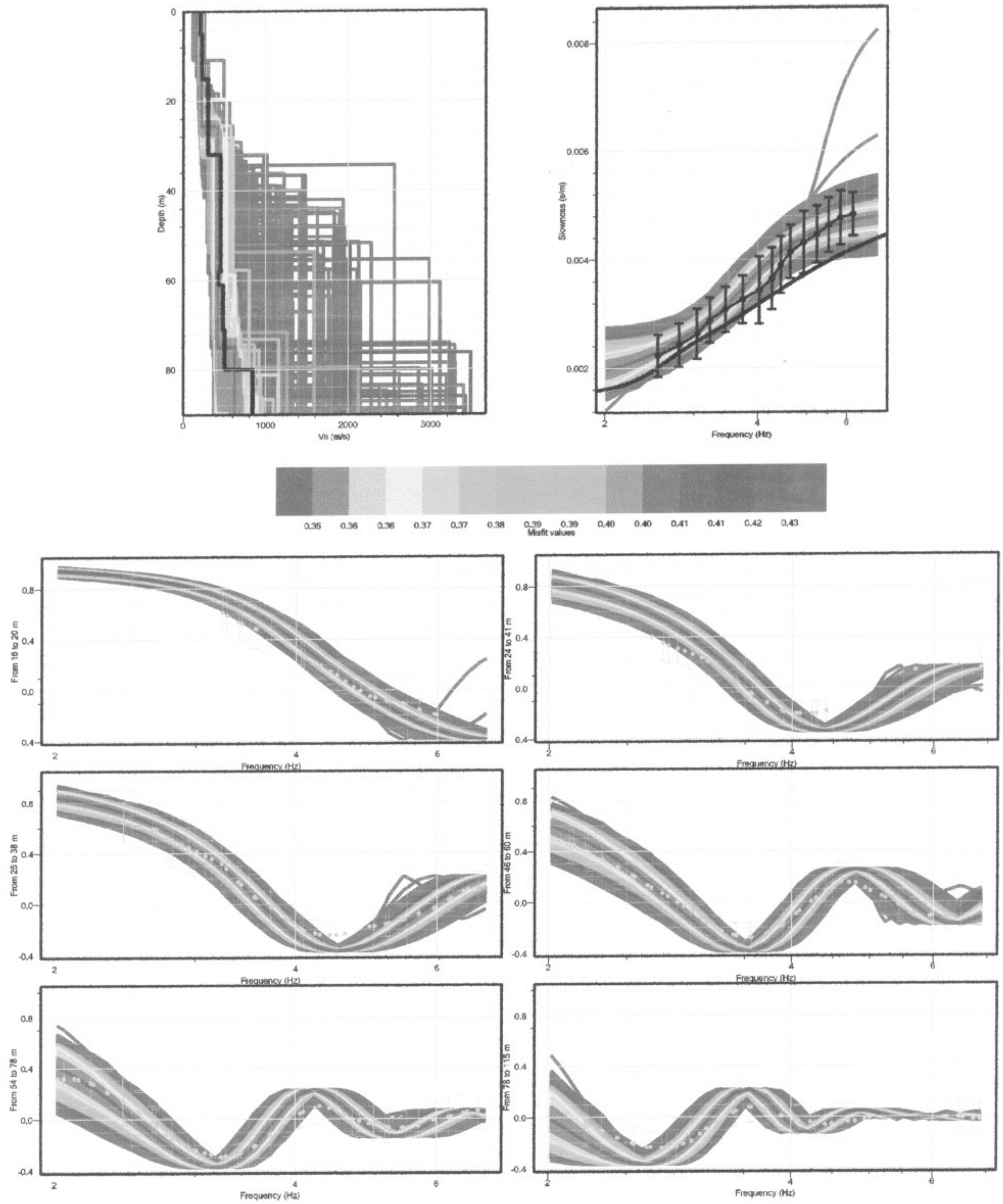

Figure 6. Resulted shear wave velocity model (upper left) from the inversion of the autocorrelation curves (lower part). The shear wave velocity model from CH data and its respective DC is also presented with continuous black line. The DC from the CVFK analysis is

also given (upper right),(Vartholomio).

There is a good correlation o $h_{min1,2}$ and Ds_o for sites Aigio, Korinthos, Lefkas, Vartholomio and with D_{s1} for Pirgos. Additionally, there is a good correlation on Vs_o between array and CH shear wave velocities for Aigio, Korinthos, Lefkas, Vartholomio and Patras (only for the four layer models with a low velocity zone on the third layer). Finally concerning the correlation of Ds_o and Ds_1 there is a high dependence on the parameter space used (two, three layer models) and differs from site to site if it is high with Ds_o or Ds_1.

6. Conclusions

The application of array microtremor data in six sites of the National Strong Motion Network has been evaluated through this work and its correlation with cross-hole results and H/V spectral ratio results from earthquake data.

Two processing methods have been applied to array data, CVFK and MSPAC, and further inversion of data showed that both methods could reveal satisfactorily shear wave velocity of the first layer (Vs_o) in most sites. However, when comparing the depth of the first layer (Ds_o) or the depth of the seismic bedrock (Ds_1) with the cross-hole results coherence is of medium quality showing no processing method dependence but site and parameter space (number of layer) dependence.

The depth of the first layer matches very well the one calculated using Vs_o and the fundamental frequency considered from H/V spectral ratios of ambient noise and earthquake data ($f(hv_1)$ $f(hv)_2$) (Table I).

This is a preliminary effort and certainly it is necessary to further check the validity of array microtremor method with other geophysical methods as well in order to use it for site characterization.

7. Acknowledgments

This work has been financially supported by the France–Greek (2005-2007) bilateral cooperation project.

8. References

Aki, K. (1957) Space and time spectra of stationary stochastic waves, with special reference to microtremors, *Bulletin of Earthquake Research Institute* Tokyo Univ. 35, 415-456.

Anastasiadis, A., M. Dimosthenous, B. Lekidis, B. Margaris, A. Savvaidis, I. Sous, I. Kalogeras, I. Baskoutas, and M. Kourouzidis. The earthquake of Vartholomio (M=5.6), 2 December 2002, Strong ground motion, and structures behaviour, *Technical Chamber of Greece* Athens, 61 pp (in Greek), (2003).

Anastasiadis, A. Report on local soil site conditions of geomorphology and dynamic interactions of soil-foundation-structure on earthquake recordings of the National Strong Motion Network, *Internal Report* 6 Volumes (in Greek) (2004).

Athanassopoulos, G., P., Pelekis, and E.A. Leonidou (1999). Effects of surface topography on seismic ground response in the Egion (Greece) 15 June 1995 earthquake. *Soil Dynamic and Earthquake Engineering* 18 (2), 135-149.

Arai, H. and K. Tokimatsu (2004). S-Wave Velocity Profiling by Inversion of Microtremor H/V Spectrum. *Bulletin of the Seismological Society of America* 94 (1), 53–63.

Bard, P.-Y. (1998). Microtremor measurements: a tool for site effect estimation?, State-of-the art paper, Irikura K., Kudo K., Okada H., and Satasini T., Editors. *Effects of Surface Geology on Seismic Motion* Yokohama, Rotterdam, Balkema, 3, 1251-1279.

Bettig, B., P.-Y. Bard, F. Scherbaum, J. Riepl and F. Cotton (2003). Analysis of dense array noise measurements using the modified spatial auto-correlation method (SPAC). Application to the Grenoble area. *Bolletino di Geofisica Teorica ed Applicata* 42 (3/4), 281-304.

Table I. Results of processing and inversion of array microtremor, earthquake data and cross-hole results (detailed description on the text).

		TEAM A										TEAM B														H/V		TEAM A		TEAM B		TEAM A			TEAM B	
																																Vs0	Ds0	Ds1	Vs0	Ds0
site	method	Freq (Hz)	model	vs0-	vs0+	vs0	vs0- mean	vs0+ mean	vs0 mean	limit of the Vs0 in %	Spread of Data	DC	Freq (Hz)	model	Lowest Misfit	Vs0-	Vs0+	Vs0	Vs0- mean	Vs0+ mean	Vs0 mean	limit of the Vs0 in %	Spread of Data	Ds0	Ds1	f(hv)1 NOISE	f(hv)2 Strong Motion	hmin1 [m] NOISE	hmin2 [m] Strong Motion	hmin1 [m] NOISE	hmin2 [m] Strong Motion	Coherence Between Array and CH (0:poor-2:good)			Coherence Between Array CH (0:poor-2:	
Aigio	fk		2l	375	500	440	258	415	330	26	1.09	DCr	7-16	2l	0.364	400	550	475	322	509	403	26.16	0.86	23		5.6	1.7	15	49	18	59	2.0	1.0		2.0	1.5
			2l grad	140	330	220						very small differences between DC's		1pl+1l	0.1385	204	510	300						26								1.5	1.0		2.0	
														3l	0.0745	365	525	435						12	53										2.0	0.0
												DC1r	7-16	2l	0.3068	385	535	465						22											2.0	
														1pl+1l	0.1252	218	408	295						24											2.0	
														3l	0.0872	360	525	450						15	53										2.0	1.0
Korinthos	fk		2l	220	310	250	171	273	218	25	0.8736	DCr	5-20	2l	0.1543	210	275	255	189	263	244	22.54	0.41	19		0.32	3.5	170	16	191	17	2.0	0.0		2.0	
			2l grad	120	260	190								3lay	0.14	175	275	257						19	74							1.5	0.0		2.0	2.0
														1pl+1l	0.141	182	239	220						21											2.0	
	spac		2l	225	300	260																										2.0	0.0			
			2l grad	120	220	170																										1.5	0.0			
Lefkas	fk		2l	200	300	240	146	298	206	44	1.503	DCr	3.5-10	2l					126	267	208	39.58	1.03			2.5	3	21	17	21	17	2.0	1.0			
			2l grad	100	210	155								3l	0.175	98	242	208						12	100							1.5	1.5		2.0	0.0
														4l	0.192	143	247	207						19	69										2.0	1.0
												DC1r	3.4-7.6	3l	0.076	136	313	209						19	68										2.0	1.0
	spac		2l	195	400	280																										2.0	1.0			
			2l grad	90	280	150																										1.5	1.5			
Vartholomio	fk		2l	130	260	200	95	210	138	53	1.4545	DC1r	2.5-6.2	2l	0.158	190	240	218	172	240	208	17.21	0.48	18		1.5	1.6	23	21	35	33	2.0	0.0	0.0	2.0	
			2l grad	60	160	75								3l	0.113	167	240	202						20	80							1.0	0.0	0.0	2.0	
	spac		2l									final	1-10	2l	0.368	180	255	225						24											2.0	
			2l grad											3l	0.368	169	250	220						23	168										2.0	
												final1	2-7	3l	0.354	155	215	175						28	80										2.0	
Pirgos	fk	4.3-20	2l				248	420	320	31	0.7656	DCr	4-20	2l	0.308	365	490	431	279	505	382	32.36	0.92	12		1.3	1.2	62	67	73	80	1.0	1.0		0.0	
			2l grad	235	360	280								3l	0.099	270	500	360						6	76										1.0	
														4l	0.1	225	505	346						7	75										1.0	
												DC1r	4-20	2l	0.346	385	510	455						16											0.0	2.0
														3l	0.134	270	513	368						8	74										1.0	
														4l	0.104	160	513	330						7	55										1.0	
	spac	1.93-13	2l																																	
			2l grad	260	480	360																										1.0	1.0			
Patras 2	fk	1.74-5	2l				165	405	250	62	1.24	DCr	2-20	3l-2LV	0.57	178	805	490	225	536	365	46.74	1.95	8.00	104	0.32	3.5	195	18	285	26	1.0			0.0	
			2l grad	150	350	200								4l-3LV	0.368	183	505	260						7	31										2.0	
														4l-3LVA	0.53	93	450	313						10	110										2.0	
												DC1r	2-20	2l	0.066	346	486	384						68											0.0	
														3l	0.076	325	435	380						68	180										0.0	
	spac	0.45-5.7	2l																													1.5				
			2l grad	180	460	300																														

Borcherdt, R.D. (1970). Effects of local geological conditions in the San Francisco Bay region on ground motions and the intensities of the 1906 earthquake. *Bulletin of the Seismological Society of America* 60, 29-61.

Campbell, K.W. (1976). A note on the distribution of earthquake damage in Long Beach, 1933. *Bulletin of the Seismological Society of America* 66, 1001-1006.

Dimitriou, P., N., Theodoulidis, B. Margaris, Ch. Papaioannou, A. Savvaidis, A. Ananstasiadis, K. Klimis, K. Makra, M. Dimosthenous, Ch. Karakostas, B. Lekidis, T. Makarios, Th. Salonikios, and I. Sous (2004). The earthquake of Lefkas (M=6.2), 14th of August 2003, Strong Ground Motion, consequences of the earthquake in the building and natural environment, *Technical Chamber of Greece* Athens, 78 pages, (in Greek) (2004).

Fäh, D., F. Kind and D. Giardini (2001). Inversion of local S-wave velocity structures from average H/V ratios, and their use for the estimation of site effects, *Journal of Seismology* 7 (4), 449-467.

Hartzell, S., A. Leeds, A. Frankel, and J.Michael (1996). Site response for urban Los Angeles using aftershocks of the Northridge earthquake". *Bulletin of the Seismological Society of America* 86 (1B), S168-S192.

Ishida, H., T. Nozawa, and M. Niwa (1998). Estimation of deep surface structure based on phase velocities and spectral ratios of long-period microtremors. Irikura K., Kudo K., Okada H., and Satasini T., Editors. *Effects of Surface Geology on Seismic Motion* Yokohama, Rotterdam, Balkema, 697–704.

Konno, K., and T. Ohmachi (1998). Ground-motion characteristics estimated from spectral ratio between horizontal and vertical components of microtremor, *Bulletin of the Seismological Society of America* 88, (1), 228–241.

Kvaerna, T., and F. Ringdahl (1986). Stability of various f-k estimation techniques. Semmiannual technical summary, 1 October 1985 – 31 March 1986, *NORSAR Scientific Report* 1-86/87, Kjeller, Norway, 29-40.

Pitilakis, K. Report on effects of local soil conditions of geomorphology and dynamic interaction soil-foundation-structure on earthquake recordings of the National Strong Motion Network, *Internal Report* 8 Volumes, (in Greek) (1996).

Sambridge, M. (1999a) Geophysical inversion with a neighbourhood algorithm –I. Searching a parameter space, *Geophysical Journal International* 138, 479-494.

Sambridge, M. (1999b). Geophysical inversion with a neighbourhood algorithm – II. Appraising the ensemble, *Geophysical Journal International* 138, 727-746.

Scherbaum, F., K.-G. Hinzen, and M. Ohrnberger (2003). Determination of shallow shear wave velocity profiles in the Cologne, Germany area using ambient vibrations. *Geophysical Journal International* 152, 597-612.

SESAME European project (2004a). JSESAME user manual, Version 1.08.

SESAME European Project (2004b). Site EffectS assessment using AMbient Excitations. http://sesame-fp5.obs.ujf-grenoble.fr

Theodulidis, N., P., P. Dimitriu, and A. Savvaidis (2006). Horizontal-to-vertical spectral ratio for site characterization: The case of strong motion network in Greece (to be submitted for publication).

Tokimatsu, K. (1997). Geotechnical site characterization using surface waves. Ishiliara, Editor. *Earthquake Geotechnical Engineering,* Rotterdam, Balkema, 1333-1368.

Wathelet, M., D. Jongmans, and M. Ohrnberger (2004). Surface wave inversion using a direct search algorithm and its application to ambient vibration measurements, *Near Surface Geophysics* 2 (4), 211-222.

Wathelet, M., D. Jongmans, and M. Ohrnberger (2005). Direct Inversion of Spatial Autocorrelation Curves with the Neighborhood Agorithm, *Bulletin of the Seismological Society of America* 95 (5), 1787-1800.

Yamanaka, H. (1998), Geophysical explorations of sedimentary structures and their characterization. Irikura K., Kudo K., Okada H., and Satasini T., Editors. *The Effects of Surface Geology on Seismic Motion*, Rotterdam, Balkema, 15-33.